JB Accepts, published online ahead of print on 7 September 2012
J. Bacteriol. doi:10.1128/JB.01291-12

Directional Evolution of *Chlamydia trachomatis* Towards Niche-specific Adaptation

Running title: Chlamydia trachomatis adaptive evolution

Vítor Borges [a], Alexandra Nunes [a], Rita Ferreira [a], Maria J. Borrego [a], and João P. Gomes [a,*]

[a] Department of Infectious Diseases, National Institute of Health, Av. Padre Cruz, 1649-016 - Lisbon, Portugal

[*] Corresponding author: J.P. Gomes

Address: Department of Infectious Diseases, National Institute of Health, Av. Padre Cruz, 1649-016 - Lisbon, Portugal; Tel.: (+315) 217 519 241; fax: (+351) 217 526 400; E-mail address: j.paulo.gomes@insa.min-saude.pt

ABSTRACT

On behalf of host–pathogen arms race, a cutting-edge approach for elucidating genotype-phenotype relationships relies on the identification of positively selected *loci* involved in the pathoadaptation. We studied the obligate intracellular bacterium *Chlamydia trachomatis*, for which same-species strains display a nearly identical core and pan genome, while presenting a wide range of tissue tropism and ecological success. We aimed to evaluate the evolutionary patterns underlying species separation (divergence) and *C. trachomatis* serovar radiation (polymorphism), and to establish genotype/phenotype associations. By analyzing 60 *Chlamydia* strains, we detected traces of Muller's ratchet as a result of speciation, and identified positively selected genes and codons hypothetically involved in infection of different human cell types: columnar epithelial cells of ocular or genital mucosae, and mononuclear phagocytes; and also, events likely driving pathogenic and ecological success dissimilarities. In general, these genes code for proteins involved in immune response elicitation, proteolysis, subversion of host-cell functions, and also proteins with unknown function. Several genes are potentially involved in more than one adaptive process, suggesting multiple functions or a distinct *modus operandi* for a specific function, and thus should be considered as crucial research targets. Additionally, six out of the nine genes encoding the putative antigens/adhesins polymorphic membrane proteins seem to be under positive selection along specific serovars, which sustains an essential biological role of this extra-large paralogues family in chlamydial pathobiology. This study provides insight into how evolutionary inferences illuminate ecological processes such as adaptation to different niches, pathogenicity, or ecological success driven by arms races.

INTRODUCTION

Genomic changes of microbial pathogens are directly linked to the evolutionary arms race that takes place between microbe and host during the infectious process, as a result of the antagonistic interaction, and they are a consequence of polymorphisms accumulated after selective pressure from the host's inflammatory or immune response (32). However, the majority of coding genes present a higher number of synonymous rather than non-synonymous substitutions, which indicates that purifying selection is operating to preserve the current function and structure of the protein, and only a small fraction of the genes are expected to be positively selected where diversification is favored through increased fitness (11). In order to understand the evolutionary forces that act on gene variation, major challenges are to identify *loci* that might have been under selection, and to determine the type of natural selection that has influenced their evolutionary history (59). In the field of infectious diseases, site-specific inferences regarding positive selection on *loci* involved in drug resistance (19) or in the interaction with the host immune system have been proposed as complementary approaches for the development of vaccines against HIV and other viruses (33), and also to predict the evolution of virulent strains of the influenza virus (12). Also, it has been shown that core genes are equally subjected to positive selection as pathogen specific accessory genes (4), suggesting that blind genomic-scale analysis should be performed.

For a species such as *Chlamydia trachomatis* with a wide range of tissue tropism and ecological success, but presenting a nearly identical core and pan genome, and a DNA sequence similarity of > 98% (39), the few existing polymorphisms are expected to be extremely informative of the adaptive evolution process. However, an excess of nonsynonymous substitutions alone is not sufficient to invoke positive selection, as it requires an increase in fitness caused by the corresponding amino-acid replacement. Otherwise, it may represent the accumulation of slightly deleterious mutations (not severe

deleterious as these will not become fixed because they render their bearers non-viable) to the pathogen on behalf of the Muller's ratchet theory (27, 60). This is predicted to operate in intracellular replicating bacteria (as *C. trachomatis,* which replicates within a host vacuole named inclusion) that are subject to recurrent bottlenecks and replicate in small populations, with little opportunity for recombination and few back or compensatory mutations (2). Although it was recently shown (39) that recombination events affect much more chromosome regions than previous suspected in *C. trachomatis*, the frequency and the relative weight of recombination and mutation calculated for this pathogen ($\rho/\theta < 0.07$ and $r/m < 0.71$, respectively) (28, 49) indicates the point mutation events as the major evolutionary driving force.

In the present study, we used comparative genomics over 59 *C. trachomatis* strains (comprising all serovars) to clarify the mutational dynamics underlying both the separation of *C. trachomatis* as species, and the pathoadaptation driven by arms race. We identified positively selected genes and codons that are hypothetically involved in the evolutionary adaptation of *C. trachomatis* serovars to different cell types: mucosal cells from the eye conjunctiva (responsible for trachoma) (serovars A-C), from the genitalia (primarily yielding cervicitis) (serovars D-K), and mononuclear phagocytes (yielding invasive diseases such as hemorrhagic proctitis and suppurative lymphadenitis) (serovars L1-L3). Finally, we also detected positive selection events likely driving pathogenic and ecological success dissimilarities.

MATERIAL AND METHODS

***C. trachomatis* strains, cell culture and DNA extraction.** The present study encompasses data from 59 *C. trachomatis* strains and the *Chlamydia muridarum* Nigg strain (also called, Mouse Pneumonitis strain – MoPn) (listed in the Table S1). These include *in silico* data from recently

93 analyzed fully-sequenced *C. trachomatis* strains (39) and eight historical prototype strains (Ba/Apache-
94 2, C/TW3, F/IC-Cal3, G/UW57, H/UW43, I/UW12, J/UW36 and K/UW31) in order to enroll all the 15
95 major serovars. Those additional eight strains were propagated in HeLa 229 cell monolayers and at 48
96 to 72 hours post-infection, cells were harvested and a bacteria-enriched pellet was obtained and
97 resuspended in 200 µl of PBS, as previously described (9). DNA was extracted using the QIAamp®
98 DNA Mini Kit (Qiagen) according to manufacturer's instructions, and stored at -80 ºC until use.

99 **Selection of *loci* and sequencing.** Based on available *in silico* full-genome sequence data, we
100 searched for polymorphic genes among *C. trachomatis* strains through the progressiveMauve algorithm
101 (23) of the Mauve software v2.3.1. A detailed evaluation of polymorphism of each *locus* was further
102 performed by using Lasergene® 9.0. (DNASTAR, Madison, Wisconsin, USA) and MEGA5 (76).
103 Chromosome *loci* revealing an extremely low polymorphism were discarded from the present analysis
104 as their use would hamper the accurate application of likelihood tests. We ended up with 75 top-ranked
105 polymorphic genes (listed in the Table S2). These were categorized according to their functional role,
106 involving 20 housekeeping genes (HKs), 14 genes encoding well-known cell envelope proteins (CEPs),
107 31 genes coding for secreted proteins (SECs), and 10 genes coding for proteins with unknown function
108 or for which the biological role is not consensual. The SEC category involves proteins secreted [either
109 by the Type III Secretion System (T3SS) - a machinery used by many bacterial pathogens to
110 manipulate eukaryotic host cells by injecting virulence proteins - or by an undefined mechanism], into
111 the cytosol of the host cells or to the inclusion membrane. For analyses enrolling divergence *versus*
112 polymorphism, the corresponding orthologous genes of the *Chlamydia muridarum* Nigg strain were
113 identified (by NCBI-BLAST search) and sequences were collected from the full-genome annotated in
114 the GenBank database (accession number NC_002620) (65). For the strains that we needed to
115 propagate as no *in silico* data was available, the 75 genes were amplified and sequenced by using

standard procedures (36). The sequences and location of primers, as well as the amplicon sizes are listed in the Table S3. Automated sequencing was achieved using BigDye Terminator v1.1 Cycle Sequencing chemistry, according to the manufacturer's instructions (Applied Biosystems) in an Applied Biosystems 3130*xl* Genetic Analyzer. Sequence reads were assembled using SeqBuilder software (DNASTAR) and alignments were generated using the ClustalW algorithm implemented in both the MegAlign software (DNASTAR) and MEGA5. A concatenated alignment of the 75 genes was also constructed for all *C. trachomatis* and *C. muridarum* strains. As the ClustalW program generates alignment artifacts in the presence of insertion/deletion (indel) events by disrupting codons, we edited "by hand" the amino acid alignments rather than only automate the process before editing the corresponding nucleotide sequences. When strain-exclusive single nucleotide polymorphisms (SNPs), indel events and pseudogenes were identified, resequencing was performed from a newly extracted DNA, and new sequences reads were generated for comparative purposes.

Phylogenomic analysis. Analyses of genetic diversity and phylogeny were conducted for each gene by using MEGA5. Briefly, we computed overall mean distances (number of differences and p-distance) and matrices of pairwise comparisons at both nucleotide and amino acid levels. For phylogenetic analysis, individual trees were generated using the Neighbor-Joining method with bootstrapping (67) and the evolutionary distances were computed using the Kimura 2-parameter method (52). For all these analyses, the pairwise-deletion option was selected as it excludes sites containing alignment gaps or missing data from the analysis only when necessary in the pairwise distance estimation. Truncated genes, which are expected to encode non-functional proteins, were excluded from the phylogenetic and evolutionary analyses, except for the strains with non-disrupted sequences, as their biological role may be phenotype specific.

Global analysis of molecular evolution. The nonsynonymous/synonymous substitution rate ratio (d_N/d_S) among related protein-coding DNA sequences, where d_N refers to the number of nonsynonymous substitutions per nonsynonymous site and d_S is defined as the number of synonymous substitutions per synonymous site, may be suggestive of the selective pressures driving the mutational trends (86). Initially, for a global analysis of these trends, we estimated d_N and d_S values with MEGA5 by using the Kumar model (61). For each gene, d_N/d_S was calculated over all C. *trachomatis* sequence pairs and between the sequences of the two species (*C. trachomatis* and *C. muridarum*). More, in order to reinforce the comparison between the amount of evolutionary variation within the *C. trachomatis* species (polymorphism) and the variation between *C. trachomatis* and *C. muridarum* (divergence), we also applied the McDonald-Kreitman (MK) test (26, 55). However, as it has been assumed that the results from the MK test cannot directly discriminate the type of selection acting on genes (62), the subjacent MK test algorithm was only used to clarify the neutral and amino acid-altering mutational trends underlying the *C. trachomatis* speciation process. This kind of analysis is suitable for tracing the Muller's ratchet phenomenon, which is commonly observed in niche-restricted pathogens.

Evaluation of the directionality in *C. trachomatis* evolution. In order to search for genes on which positive selection putatively operates, two distinct approaches were applied. First, as a statistical support of the d_N and d_S estimations within *C. trachomatis* strains, the codon-based Z-test of selection was computed by MEGA5 using the Kumar method (61), where bootstrapping (1000 replicates) was used for estimation of the variation in the statistic test. This test calculates the probability of rejecting the null hypothesis of strict-neutrality ($d_N = d_S$) in favor of one of two alternative hypothesis: positive selection ($d_N > d_S$) or purifying selection ($d_N < d_S$). Results with p-values less than 0.05 were considered significant at the 5% level. On a second approach, the branch-site test of positive selection (branch-site test 2) (85, 88) was employed using the *codeml* application from the Phylogenetic Analysis

by Maximum Likelihood (PAML) package (version 4.4d) (83). Alignments of nucleotide sequences from the 59 *C. trachomatis* strains and *C. muridarum* (built and corrected on MEGA5) were converted into the "interleaved" PHYLIP format using the BioEdit package (version 7.0.0) (http://www.mbio.ncsu.edu/bioedit/bioedit.html), where stop codons were removed from sequences. The branch-site test is a robust bioinformatic approach (84) that is recommended to infer positive selection in a lineage of interest (called foreground lineage) when several lineages in the phylogeny may have been subjected to distinct selective pressures (85, 88). The statistical significance of the presence of positive selection along the branch of interest was addressed by the likelihood-ratio test (LRT) (82). In the branch-site test 2, the LRT compares the twice of the log likelihood difference ($2\Delta l$) between two models (alternative and null models) with the chi-square distribution with one degree of freedom for p-value calculation (88). The alternative model allows positive selection ($d_N/d_S \geq 1$) for the foreground branch, whereas the null model assumes the d_N/d_S ratios < 1 or $= 1$ for all site classes in all branches in the phylogeny. When positive selection acting on a specific gene was suggested by a significant LRT (p-value less than 0.05), the Bayes empirical Bayes analysis (87) was used to identify the specific positively selected sites within that gene along the foreground branches. Therefore, the branch-site model requires an *a priori* definition and labeling of the foreground branches to be tested for positive selection, which should rely on well-defined biological hypotheses (85). Thus, based on the assumption that some genes might be involved in *C. trachomatis* phenotypic dissimilarities as a result of targeted positive selective pressures, we created six comprehensible biological hypotheses (H1-H6). The hypotheses evaluate the existence of genes under positive selection that may be involved in the following biological processes: specific cell-appetence to columnar epithelial cells of ocular (H1) or genital mucosae (H2), and to mononuclear phagocytes (H3); pathogenic diversity among strains causing ocular disease (H4), genital disease (H5), or hemorrhagic proctitis and suppurative

lymphadenitis (H6). Only the genes for which the phylogeny supported any of these scientific hypotheses were tested.

Finally, as recombination may bias the results of positive selection, we used published data on recombination analysis enrolling all *C. trachomatis* genes (39, 41, 49) to inspect whether the genes selected for the present study showed evidences of recombination. Consequently, for the genes showing incongruent trees where unequivocal recombination was detected within a specific branch, the analysis of positive selection was excluded *a priori* for the corresponding biological hypothesis. On the other hand, genes yielding congruent trees but for which recombination had been previously detected (39, 41, 49) were still subjected to positive selection analysis and are properly identified in the present study.

Nucleotide sequences accession number. The nucleotide sequences determined in the present study were submitted to the GenBank database (http://www.ncbi.nlm.nih.gov/Genbank/index.html) and are currently available for consulting through the accession numbers: JQ066324 - JQ066722.

RESULTS

Polymorphism significance of the selected genes. Distribution of point mutations in *C. trachomatis* chromosome is highly heterogeneous. Although the selected genes (Fig. 1 and Table S2) represent 11% of the coding region length, they encompass about 55% of all chromosomal SNPs occurring within coding regions, which corresponds to a total of 5083 polymorphic sites among the 59 strains. In fact, we found that any given chromosomal SNP has 10.0 (odds ratio, 95% CI: 9.3 - 10.7) times higher probability to belong to the pool of genes under evaluation than to show up in any other gene (Fisher's exact test, $p < 10^{-7}$).

Divergence *versus* polymorphism – detection of Muller's ratchet. Considering that *C. trachomatis* and *C. muridarum* species evolved from a last common ancestor (65), the comparison between the amount of evolutionary variation within the *C. trachomatis* species (polymorphism) and between *C. trachomatis* and *C. muridarum* (divergence) may shed some light on the evolutionary mutational dynamics that drove the *C. trachomatis* speciation. Accordingly, the divergence of the two species was evaluated through estimation of the d_N/d_S ratio between orthologous genes. All genes revealed d_N/d_S values lower than one, where the mean value was 0.21 (standard deviation (SD), 0.14) (Fig. 2). This observation suggests an unequivocal higher weight of synonymous than nonsynonymous changes on the species divergence, in agreement with the neutral theory of molecular evolution (53), which postulates that the fixation of selectively neutral mutations by random genetic drift is the major factor responsible for species divergence.

Subsequently, we compared these results with the d_N/d_S values obtained solely within *C. trachomatis* species (i.e., among the 59 strains). We observed that there was a high, but dissimilar, decrease of both d_S and d_N values after the separation of the two species from a common ancestor (Fig. 2). In fact, the observed mean of the decay of d_S values [147.2 (SD±243.7)] was 5.5 times higher than the one observed for d_N [26.9 (SD±19.9)]. This was a consistent trend as the McDonald-Kreitman test algorithm yielded a similar decays ratio of 4.7. Globally, this suggests that, since *C. trachomatis* was established as species, the nonsynonymous changes increased their relative weight to synonymous changes in contrast with the evolutionary process that originated the separation of the two species. This observation is consistent with the Muller´s ratchet theory (27, 60) which assumes an accumulation of slightly deleterious non-silent mutations on microbial populations repeatedly subjected to genetic bottlenecks. In fact, the obligate intracellular lifestyle of *C. trachomatis*, which is characterized by niche-restricted and low-size populations, and expected low frequency of recombination relative to

229 mutation events (28, 49), may lead to less effective elimination and consequent accumulation of non-
230 silent mutations (2).

231 **Evolutionary trends within the *C. trachomatis* species.** We further focused on studying the
232 accumulation of mutations after *C. trachomatis* speciation, with special emphasis on protein-altering
233 changes that have contributed for phenotype divergences, which may help to clarify the *C. trachomatis*
234 niche-specific adaptation. For each gene, the d_N/d_S ratio was evaluated over all C. *trachomatis*
235 sequence pairs (Fig. 3), where genes exhibiting d_N/d_S ratios above 1 and a significant p-value (<0.05) in
236 the codon-based Z-test of positive selection ($d_N/d_S > 1$) were considered as putative targets of positive
237 selection. Twenty-seven genes exhibited overall d_N/d_S values higher than one, in which 15 (including
238 14 SECs) revealed a significant Z-test p-value. As predicted, all housekeeping genes presented d_N/d_S
239 ratios below one, which indicates that the genes involved in regulatory/metabolic functions are less
240 likely targeted by diversifying selection (47). On the other hand, 22 out of the 31 SECs support an
241 opposite scenario, which is relevant as these proteins contact directly with the host, and thus are more
242 prone to be involved in pathoadaptation. We also investigated if the types of mutation are dependent on
243 the degree of genetic variability by evaluating the relationship between d_N and d_S values and the
244 nucleotide polymorphism (p-distance) among *C. trachomatis* strains (Fig. 4). Globally, as observed
245 above for species divergence, we found that the increment in polymorphism is essentially driven by
246 fixation of silent mutations, which presented an increase rate about four-fold higher than non-silent
247 changes.

248 **Distribution of d_N and d_S *versus* disease outcomes and ecological success.** We also aimed to
249 understand if the general distribution of both silent and non-silent mutations among *C. trachomatis*
250 corresponds to strains clustering by disease outcomes. We used the concatenated sequences
251 encompassing all genes under evaluation to calculate the d_N and d_S distances between each strain and

the different groups of strains (i.e., three disease groups) (Fig. 5). Our results sustain a non-random accumulation of mutations where strains with the same cell-appetence are unequivocally clustered either by silent mutations or protein-changing alterations. Indeed, the genetic distances between strains with dissimilar tropism are 1.8- to 10.5-fold (for d_S) and 1.7- to 6.7-fold (for d_N) higher than the ones between strains with similar cell-appetence. Additionally, the highly ecological succeeded strains causing non-invasive genital infections (mostly from serovars E and F) are slightly separated from the remainder genital strains (Fig. 5). This analysis clearly supports that our approach for detecting positively selected genes (and codons) relying on rationally established biological hypotheses (see methods) may be an useful step for understanding the molecular basis underlying *C. trachomatis* phenotypic differences.

Positive selection driving bacterial specific appetence to different human cell types. The phylogenetic analysis revealed genes whose trees cluster all strains that preferentially infect the same human cell type in a single branch. Thus, genes (and codons) targeted by positive selection along those branches may be involved on specific host-cell interactions. To evaluate this, we conducted the branch-site test of positive selection under the biological hypotheses H1 to H3 (see methods). All genes and the inferred positively selected codons found to be putatively involved in specific adaptive processes are described in Fig. 6 and Table 1. Five genes were found to be under positive selection in the evolutionary process that drove the segregation of ocular strains (branch H1). These include genes encoding two polymorphic membrane proteins (Pmps) (CT869/*pmpE* and CT870/*pmpF*), one Pmp-like protein (CT050), one inclusion membrane protein (Inc) (CT115/*incD*) and the translocated actin recruiting phosphoprotein (CT456/*tarp*). The Pmps and Incs are among the most promising research targets for which there is cumulative evidence of their involvement in biological mechanisms such as adhesion, immune response elicitation, or subversion of intracellular trafficking (see Table 1 for

details) (21, 25, 35, 38, 66, 68, 78). For example, PmpF was predicted *in silico* to contain T-cell epitopes that bind HLA class I and II alleles (15). On the other hand, Tarp is a chlamydial effector of the T3SS associated with the chlamydial invasion of the host cells (44) by mediating host actin polymerization and inclusion development (20, 42).

For the biological hypothesis H2, we found significant evidence supporting a fixation of adaptive mutations driving a better appetence to the columnar epithelial cells of genital mucosa (branch H2) solely for the gene CT105. Although its function is unknown, a previous study of heterologous expression in yeast (71) suggested that CT105 may be involved in modulation of host cellular functions. Nevertheless, it is worth to note that CT105 is a pseudogene for ocular strains, thus we may be facing a scenario of a gene strictly needed for tropism functions other than those involving the ocular conjunctiva. The frequent tree incongruence involving genital strains hampered the evaluation of several genes for this specific biological hypothesis (Table 1).

Regarding the branch that clusters all strains infecting the mononuclear phagocytes (branch H3), we detected 18 genes likely under positive selection. This set includes one HK, and genes encoding 11 SECs (seven Incs), four CEPs (including three Pmps), and two proteins with unknown function (Table 1). Besides the general relevance of Incs and Pmps (explained above), we would highlight the SEC CT223, an Inc protein for which it was suggested a role in subversion of host cell functions, either by containing SNARE-like (eukaryotic soluble N-ethylmaleimide-sensitive attachment protein receptors) motifs (impact in intracellular trafficking) (25), or by blocking host cell cytokinesis (1). The SECs CT622 is an antigen putatively secreted by the T3SS (21, 30, 37), whereas CT867 and CT868 are proteases that possess deubiquitinating and deneddylating activities (57), which may suggest a role in virulence. The invasive infection pattern of L1-L3 strains along with the expectation that these strains were the first to diverge from a common *C. trachomatis* ancestor (73) may justify the

high number of genes detected under diversifying selection on branch H3 rather than on branches H1 and H2. These genes may play a role in the specificity of mononuclear phagocytes-bacteria interactions that yield invasive infections with L1-L3 strains.

Positive selection driving pathogenic diversity among strains infecting the same human cell type. The detection of positive selection acting on specific genes along branches of strains causing similar disease outcomes may be useful for understanding adaptive alterations underlying niche-specific pathogenic dissimilarities. Among the ocular strains, we detected two genes under positive selection (branches H4) (Fig. 6): one *pmp* (CT413/*pmpB*) and CT456/*tarp* (Table 1). CT456/*tarp* had been already indicated as potentially involved in distinct pathogenic patterns displayed by two ocular strains (both of serovar A) when infecting cynomolgus monkeys (51).

Regarding the detection of positive selection driving pathogenic differences among strains causing non-invasive urogenital disease (branches H5), we found the above described virulence factors CT223 and CT456/*tarp*, and one *pmp* (CT872/*pmpH*). Once more, the analysis of positive selection underlying pathogenicity among non-invasive genital strains was impaired by the described recombination events involving these strains (Table 1) (39, 41, 49). Of notice was the detection of positive selection events governing the evolutionary segregation of the most succeeded genital strains (mostly from E and F serovars) for the gene coding CT694. This protein is an immunodominant antigen (69), and it was also demonstrated its secretion into the host cytoplasm by the T3SS at early time-points after infection (as CT456/Tarp), where it localizes to host cell membranes and interacts with eukaryotic AHNAK, an actin-binding protein; it is believed that CT694 may act by regulating membrane fluidity or by remodeling actin filaments during invasion or early stages of *C. trachomatis* development (10, 40). Thus, differences in immune evasion strategies or in host-cell manipulation during invasion may be crucial biological processes underlying ecological success.

Despite the remarkable genomic homogeneity of *C. trachomatis* strains that infect the mononuclear phagocytes (Fig. 5), we found 11 positively selected genes along the branches embodying SNPs that distinguish these strains (branches H6). These include four *pmps* (CT413/*pmpB*, CT414/*pmpC*, CT871/*pmpG* and CT872/*pmpH*), two genes encoding Pmp-like proteins (CT050 and CT051), three genes coding for Incs (CT147, CT233/*incC* and CT442/*crpA*), CT456/*tarp* and CT868. Besides what was generally described above for these proteins, it is worth to note that the Inc CrpA (6) is a T3SS substrate (75) that may play a role in immune evasion as it was found to be targeted by CD8+ T cells in response to infection in murine (72). Also notable is that all adaptive codons inferred for the CT233/*incC* (Table 1) correspond to the IncC N-terminal domain, and, more specifically within the first 15 residues, where it is known to reside the secretion signals recognized by T3SSs (75).

Evolutionary inferences and associated bias. The branch-site test may generate some erroneous detected positively selected genes. Although this was not assessed in the present study, recent robust evaluations estimated a range of 0-5% of false positives on this test (84). Nevertheless, this is more problematic when performing inter-species analyses as it involves highly divergent sequences (5), which is not the case of the intra-species analysis performed in the present study. Furthermore, to guide against violations of model assumptions, we applied very conservative criteria to calculate p-values in the LRT by using χ_1^2 as the null distribution (5, 88). Recombination is another critical factor that may bias the estimation of positive selection. As previous data based on full-genome sequences (39, 41, 49) detected recombination for some of the genes enrolled in the present study, some specific biological hypothesis could not be subjected to the branch-site test of positive selection. These specific exclusions are indicated in the Table 1. The remainder biological hypotheses were tested as recombination is not observed in the corresponding branches. For example, for CT147 tree, where some ocular strains are shown within a genital branch (hampering the analysis of the hypotheses H1,

H2, H4, and H5), the hypotheses H3 and H6 could still be validated. In another scenario, when recombination is known to occur in genes presenting strong congruent trees (as for CT870/*pmpF*), all hypothesis were evaluated. For these specific cases (indicated in Fig. 6) the results should be eyed with caution.

DISCUSSION

A well-known metaphor in evolutionary biology is the adaptive landscape represented by a two-dimensional plot of all genotypes in a specific environment, with their fitness represented by the height of the landscape. For each new environment, in order to climb the fitness peak, bacteria will have to acquire new beneficial mutations, which will likely be differentially spread among different genotypes (80). Presumably, the radiation of *C. trachomatis* species into strains with different cell-appetence may be explained by this scenario. Indeed, the different environments are represented by the dissimilar human tissues that strains preferentially infect (ocular, genital tract and lymph nodes), which present heterogeneous properties in terms of competing flora, immune response, and physiological characteristics (such as pH and hormonal concentration). Also, strains present dissimilar fitness as serovar E and F together represent more than 40% of all genital infections worldwide (64), and serovars A and L2 clearly predominate in ocular (3) and lymphogranuloma (79) infections, respectively. On the other hand, *C. trachomatis* is an obligate intracellular bacterium with low doubling time (9) and population size (34), and is thus subjected to transmission bottlenecks which make this pathogen a target for the accumulation of deleterious mutations on behalf of the Muller's ratchet theory. The validity of the Muller's ratchet has been evaluated either in RNA viruses (18), which present high mutation rates, are subjected to recurrent bottlenecks and the rate of compensatory back-mutations is low, or even in large free-living bacteria such as *Salmonella typhimirium*, where these

367 contributing factors are clearly attenuated (2). In our study when the values of d_N and d_S are compared
368 independently, it is noticeable that, after the *C. muridarum/C. trachomatis* separation from a common
369 ancestor, the values of d_S show a 147-fold decrease whereas the values of d_N only decrease 27-times
370 (Fig. 2), which evidences the existence of an accumulation of deleterious mutations due to genetic
371 bottleneck, as postulate by Muller. We speculate that, besides this scenario, some non-silent changes
372 may reflect adaptive mutations to different niches rather than deleterious mutations specific of same-
373 niche infecting strains. Thus, the detection of positive selection events acting on particular genomic
374 regions may help to elucidate genotype-phenotype relationships. Unfortunately, there are scarce cases
375 where genotype and phenotype are unequivocally linked in *C. trachomatis*, because no straightforward
376 tools to genetically manipulate this pathogen are available so far. One of the few examples is illustrated
377 by the mutational pattern of the *trpBA* operon (encodes tryptophan synthase, which uses indole as
378 substrate), where genital strains possess an intact and active operon whereas it is truncated by point
379 mutations or small indels in strains infecting the ocular conjunctiva (where indole is rare) (13). Thus,
380 mutations that are beneficial in one genetic background are not necessarily beneficial in another
381 background. In our study, a similar scenario may stand for CT105, which is a pseudogene for the ocular
382 strains whereas our results suggest that it may be involved in the strains' appetence to the genital
383 epithelium (Fig. 6 and Table 1).

384 Our results showed that non-silent changes differentiate strains with different cell-appetence or
385 pathogenesis (Fig. 5) and involve genes whose functions may underlie distinct phenotypes. In fact,
386 among the 25 genes identified as positively selected along specific lineages (Table 1), we found genes
387 encoding proteins implicated in immune response elicitation (such as CT147, CT442/*crpA,* CT529,
388 CT694, and *pmps*) (21, 30, 31, 69, 72, 78), proteolytic activity (such as CT867 and CT868) (57), and
389 subversion of host-cell functions (such as CT223 and CT456/*tarp*) (25, 44). Some of these genes were

390 also identified in a previous study (49), but no genotype/phenotype associations could be established
391 because only six serovars were evaluated, contrarily to the present study which constitutes a
392 considerable scale-up in terms of genetic variability (enrolling all major 15 serovars represented by 59
393 strains). A detailed view of the positively selected *loci* that we have detected revealed 11 genes
394 (CT050, CT051, CT115/*incD*, CT147, CT223, CT413/*pmpB*, CT456/*tarp*, CT868, CT870/*pmpF*,
395 CT871/*pmpG* and CT872/*pmpH*) supporting two or more biological hypotheses for adaptive changes
396 (Fig. 6). Although this seems intriguing in terms of evolutionary directionality, experimental evidences
397 suggest multiple functions for some of them (Table 1) or a distinct *modus operandi* for a specific
398 function. The most striking example is illustrated by CT456 which codes for Tarp. Strong experimental
399 evidences showed that this T3SS effector is associated with the recruitment of host-cell actin observed
400 at early stages of invasion, involving a C- terminal actin binding domain (ABD) and a proline-rich
401 region (43). Whereas the invasive serovar L2 contains a single functional ABD and it is believed that
402 the proline rich domain plays also a role in actin nucleation, Tarp from strains with different cell-
403 appetence contain multiple ABD sites that are able to nucleate actin without the need of the respective
404 proline-rich domain (44). These data suggest that strains may use Tarp distinctly for actin nucleation.
405 Also, Tarp harbors an N-terminal tyrosine-rich repeat domain (the number of repeats are serovar-
406 dependent) that is tyrosine phosphorylated by host cell kinases (42). Curiously, some positively
407 selected sites found to be associated with infection of mononuclear phagocytes (Table 1) are located
408 precisely within the tyrosine-rich repeat domain. Moreover, there seems to be a pattern of amino acid
409 substitution, where positive selection is operating on exactly the same amino acid positions within the
410 repeated regions, involving always the exchange between aspartic acid (D) and glycine (G) for seven of
411 the positively selected sites (Table 1). In support of recently published data by Mehlitz and colleagues
412 (56), it can be speculated that, as for the Tarp C-terminal region, dissimilar *modus operandi* of Tarp N-

terminal region may underlie distinct phenotype properties of *C. trachomatis* strains. Also of relevance is CT868, a deubiquitinating and deneddylating enzyme that likely interferes in multiple cellular processes. Indeed, a recent study demonstrated that CT868 is capable of inhibiting the host inflammatory responses by blocking the nuclear factor-kB pathway, a known mechanism by which pathogenic microorganisms evade the host immune responses (54). Facing these data and considering the privileged representation of these 11 *loci* in the Fig. 6, they should be considered as crucial research targets to improve our knowledge in the pathobiology of *C. trachomatis*.

It is also worth notable that, among the nine-member Pmp paralogues family, six genes seem to be under positive selection for specific phenotypes. Cumulative evidences indicate that Pmps may function as fine-tune determinants of *C. trachomatis* pathobiology, either by antigenic variation (15, 21, 63, 78), or host-cell adhesion (22, 36, 38), hypothetically through a shut-off mechanism at the inclusion level (77). It is posited that the accelerated evolution between paralogues is common and constitutes a mechanism for the generation of new genes and new biochemical functions (46).

Darwinian evolution generally relies on the existence of an adaptive pathway in which intermediate steps provide a gradual improvement of fitness. Thus, adaptive changes should not completely rule out synonymous mutations. In fact, the latter may alter the immediate protein adaptive landscape (by changing the proximal amino acids), providing the protein with new opportunities to evolve (14). Also, they can change RNA secondary structure and influence its stability (17) as well as originate codons with different frequency usage (associated with tRNA abundance), which was already shown to affect the translation efficiency in several microorganisms (50, 70). We have previously shown synonymous changes to more favorable codons for the *C. trachomatis* major antigen (64), and it is reasonable to expect that several other *loci* present synonymous changes that, in a camouflaged way, become adaptive. Our results support a non-random accumulation of synonymous mutations in *C.*

436 *trachomatis*. In fact, we found that strains infecting the same human cell type are clearly the most
437 closely related through d_S analysis (Fig. 5), which suggests a non-stochastic fixation of synonymous
438 mutations.

439 As concluding remarks, our results support a directional evolution of *C. trachomatis* towards
440 niche-specific adaptation besides a background of Muller's ratchet deleterious mutations. Whereas the
441 molecular basis for organ/cell-appetence is likely complex, these data suggest that population genetics
442 and evolutionary inferences may be key factors to a comprehensive understanding of the resulting
443 phenotypes, by guiding subsequent experimental procedures to specific targets.

444

445 **ACKNOWLEDGEMENTS**

446 This work was supported by a grant, PTDC/SAU-MII/099623/2008, from Fundação para a Ciência e a
447 Tecnologia (FCT). VB and RF are recipients of Ph.D. fellowships (SFRH/BD/68527/2010 and
448 SFRH/BD/68532/2010, respectively) from FCT. AN is a recipient of a post-doctoral fellowship
449 (SFRH/BPD/75295/2010) from FCT.

450

451 **REFERENCES**

452 1. **Alzhanov DT, Weeks SK, Burnett JR, Rockey DD.** 2009. Cytokinesis is blocked in mammalian
453 cells transfected with *Chlamydia trachomatis* gene CT223. BMC Microbiol. **9:**2.
454 2. **Andersson DI, Hughes D.** 1996. Muller's ratchet decreases fitness of a DNA-based microbe. Proc.
455 Natl. Acad. Sci. U.S.A. **93:**906–907.
456 3. **Andreasen AA, Burton MJ, Holland MJ, Polley S, Faal N, Mabey DC, Bailey RL.** 2008.
457 *Chlamydia trachomatis* ompA variants in trachoma: what do they tell us? PLoS Negl. Trop. Dis.
458 **2:**e306.

4. **Anisimova M, Bielawski J, Dunn K, Yang Z.** 2007. Phylogenomic analysis of natural selection pressure in *Streptococcus* genomes. BMC Evol. Biol. **7:**154.

5. **Anisimova M, Yang Z.** 2007. Multiple hypothesis testing to detect lineages under positive selection that affects only a few sites. Mol. Biol. Evol. **24:**1219–1228.

6. **Bannantine JP, Griffiths RS, Viratyosin W, Brown WJ, Rockey DD.** 2000. A secondary structure motif predictive of protein localization to the chlamydial inclusion membrane. Cell Microbiol. **2:**35–47.

7. **Bannantine JP, Rockey DD, Hackstadt T.** 1998. Tandem genes of *Chlamydia psittaci* that encode proteins localized to the inclusion membrane. Mol. Microbiol. **28:**1017–1026.

8. **Belland RJ, Zhong G, Crane DD, Hogan D, Sturdevant D, Sharma J, Beatty WL, Caldwell HD.** 2003. Genomic transcriptional profiling of the developmental cycle of *Chlamydia trachomatis*. Proc. Natl. Acad. Sci. U.S.A. **100:**8478–8483.

9. **Borges V, Ferreira R, Nunes A, Nogueira P, Borrego MJ, Gomes JP.** 2010. Normalization strategies for real-time expression data in *Chlamydia trachomatis*. J. Microbiol. Methods 82:256–264.

10. **Bullock HD, Hower S, Fields KA.** 2012. Domain analyses reveal that *C. trachomatis* CT694 belongs to the membrane-localized family of type III effector proteins. J. Biol. Chem., in press.

11. **Bush RM.** 2001. Predicting adaptive evolution. Nat. Rev. Genet. **2:**387–392.

12. **Bush RM, Bender CA, Subbarao K, Cox NJ, Fitch WM.** 1999. Predicting the evolution of human influenza A. Science **286:**1921–1925.

13. **Caldwell HD, Wood H, Crane D, Bailey R, Jones RB, Mabey D, Maclean I, Mohammed Z, Peeling R, Roshick C, Schachter J, Solomon AW, Stamm WE, Suchland RJ, Taylor L, West SK, Quinn TC, Belland RJ, McClarty G.** 2003. Polymorphisms in *Chlamydia trachomatis*

tryptophan synthase genes differentiate between genital and ocular isolates. J. Clin. Invest. **111:**1757–1769.

14. **Cambray G, Mazel D.** 2008. Synonymous genes explore different evolutionary landscapes. PLoS Genet. **4:**e1000256.
15. **Carlson JH, Porcella SF, McClarty G, Caldwell HD.** 2005. Comparative genomic analysis of *Chlamydia trachomatis* oculotropic and genitotropic strains. Infect Immun, **73:**6407–6418.
16. **Carver T, Thomson N, Bleasby A, Berriman M, Parkhill J.** 2009. DNAPlotter: circular and linear interactive genome visualization. Bioinformatics **25:**119-120.
17. **Chamary JV, Hurst LD.** 2005. Evidence for selection on synonymous mutations affecting stability of mRNA secondary structure in mammals. Genome Biol. **6:**R75.
18. **Chao L**. 1990. Fitness of RNA virus decreased by Muller's ratchet. Nature **348:**454–455.
19. **Chen L, Perlina A, Lee CJ.** 2004. Positive selection detection in 40,000 human immunodeficiency virus (HIV) type 1 sequences automatically identifies drug resistance and positive fitness mutations in HIV protease and reverse transcriptase. J. Virol. **78:**3722–3732.
20. **Clifton DR, Fields KA, Grieshaber SS, Dooley CA, Fischer ER, Mead DJ, Carabeo RA, Hackstadt T.** 2004. A chlamydial type III translocated protein is tyrosine-phosphorylated at the site of entry and associated with recruitment of actin. Proc. Natl. Acad. Sci. U.S.A. **101:**10166-10171.
21. **Coler RN, Bhatia A, Maisonneuve JF, Probst P, Barth B, Ovendale P, Fang H, Alderson M, Lobet Y, Cohen J, Mettens P, Reed SG.** 2009. Identification and characterization of novel recombinant vaccine antigens for immunization against genital *Chlamydia trachomatis*. FEMS Immunol. Med. Microbiol. **55:**258–270.

22. **Crane DD, Carlson JH, Fischer ER, Bavoil P, Hsia RC, Tan C, Kuo CC, Caldwell HD.** 2006. *Chlamydia trachomatis* polymorphic membrane protein D is a species-common pan-neutralizing antigen. Proc. Natl. Acad. Sci. U.S.A. **103:**1894–1899.

23. **Darling AE, Mau B, Perna NT.** 2010. progressiveMauve: multiple genome alignment with gene gain, loss and rearrangement. PLoS One **5:**e11147.

24. **Dehoux P, Flores R, Dauga C, Zhong G, Subtil A.** 2011. Multi-genome identification and characterization of chlamydiae-specific type III secretion substrates: the Inc proteins. BMC Genomics **12:**109.

25. **Delevoye C, Nilges M, Dehoux P, Paumet F, Perrinet S, Dautry-Varsat A, Subtil A.** 2008. SNARE protein mimicry by an intracellular bacterium. PLoS Pathog. **4:**e1000022.

26. **Egea R, Casillas S, Barbadilla A.** 2008. Standard and generalized McDonald-Kreitman test: a website to detect selection by comparing different classes of DNA sites. Nucleic Acids Res. **36**(Web Server issue)**:**W157–62157–62162.

27. **Felsenstein J.** 1974. The evolutionary advantage of recombination. Genetics **78:**737–756.

28. **Ferreira R, Borges V, Nunes A, Nogueira PJ, Borrego MJ, Gomes JP.** 2012. Impact of loci nature on estimating recombination and mutation rates in *Chlamydia trachomatis*. G3 (Bethesda) **2:**761–768.

29. **Fields KA, Mead DJ, Dooley CA, Hackstadt T.** 2003. *Chlamydia trachomatis* type III secretion: evidence for a functional apparatus during early-cycle development. Mol. Microbiol. **48:**671–683.

30. **Finco O, Frigimelica E, Buricchi F, Petracca R, Galli G, Faenzi E, Meoni E, Bonci A, Agnusdei M, Nardelli F, Bartolini E, Scarselli M, Caproni E, Laera D, Zedda L, Skibinski D, Giovinazzi S, Bastone R, Ianni E, Cevenini R, Grandi G, Grifantini R.** 2011. Approach to

discover T- and B-cell antigens of intracellular pathogens applied to the design of *Chlamydia trachomatis* vaccines. Proc. Natl. Acad. Sci. U.S.A. **108:**9969–9974.

31. **Fling SP, Sutherland RA, Steele LN, Hess B, D'Orazio SE, Maisonneuve J, Lampe MF, Probst P, Starnbach MN.** 2001. CD8+ T cells recognize an inclusion membrane-associated protein from the vacuolar pathogen *Chlamydia trachomatis*. Proc. Natl. Acad. Sci. U.S.A. **98:**1160–1165.
32. **Fraser C, Hanage WP, Spratt BG.** 2005. Neutral microepidemic evolution of bacterial pathogens. Proc. Natl. Acad. Sci. U.S.A. **102:**1968–1973.
33. **Gaschen B, Taylor J, Yusim K, Foley B, Gao F, Lang D, Novitsky V, Haynes B, Hahn BH, Bhattacharya T, Korber B.** 2002. Diversity considerations in HIV-1 vaccine selection. Science **296:**2354–2360.
34. **Gomes JP, Borrego MJ, Atik B, Santo I, Azevedo J, Brito de Sá A, Nogueira P, Dean D.** 2006. Correlating *Chlamydia trachomatis* infectious load with urogenital ecological success and disease pathogenesis. Microbes Infect. **8:**16–26.
35. **Gomes JP, Hsia RC, Mead S, Borrego MJ, Dean D.** 2005. Immunoreactivity and differential developmental expression of known and putative *Chlamydia trachomatis* membrane proteins for biologically variant serovars representing distinct disease groups. Microbes Infect. **7:**410–420.
36. **Gomes JP, Nunes A, Bruno WJ, Borrego MJ, Florindo C, Dean D.** 2006. Polymorphisms in the nine polymorphic membrane proteins of *Chlamydia trachomatis* across all serovars: evidence for serovar Da recombination and correlation with tissue tropism. J. Bacteriol. **188:**275–286.
37. **Gong S, Lei L, Chang X, Belland R, Zhong G.** 2011. *Chlamydia trachomatis* secretion of hypothetical protein CT622 into host cell cytoplasm via a secretion pathway that can be inhibited by the type III secretion system inhibitor compound 1. Microbiology **157:**1134–1144.

549 38. **Grimwood J, Stephens RS.** 1999. Computational analysis of the polymorphic membrane protein
550 superfamily of *Chlamydia trachomatis* and *Chlamydia pneumoniae*. Microb. Comp. Genomics
551 **4:**187–201.
552 39. **Harris SR, Clarke IN, Seth-Smith HM, Solomon AW, Cutcliffe LT, Marsh P, Skilton RJ,**
553 **Holland MJ, Mabey D, Peeling RW, Lewis DA, Spratt BG, Unemo M, Persson K, Bjartling**
554 **C, Brunham R, de Vries HJ, Morré SA, Speksnijder A, Bébéar CM, Clerc M, de Barbeyrac**
555 **B, Parkhill J, Thomson NR.** 2012. Whole-genome analysis of diverse *Chlamydia trachomatis*
556 strains identifies phylogenetic relationships masked by current clinical typing. Nat. Genet. **44:**413–
557 419.
558 40. **Hower S, Wolf K, Fields KA.** 2009. Evidence that CT694 is a novel *Chlamydia trachomatis* T3S
559 substrate capable of functioning during invasion or early cycle development. Mol. Microbiol.
560 **72:**1423–1437.
561 41. **Jeffrey BM, Suchland RJ, Quinn KL, Davidson JR, Stamm WE, Rockey DD.** 2010. Genome
562 sequencing of recent clinical *Chlamydia trachomatis* strains identifies loci associated with tissue
563 tropism and regions of apparent recombination. Infect. Immun. **78:**2544–2553.
564 42. **Jewett TJ, Dooley CA, Mead DJ, Hackstadt T.** 2008. *Chlamydia trachomatis* tarp is
565 phosphorylated by src family tyrosine kinases. Biochem. Biophys. Res. Commun. **371:**339–344.
566 43. **Jewett TJ, Fischer ER, Mead DJ, Hackstadt T.** 2006. Chlamydial TARP is a bacterial nucleator
567 of actin. Proc. Natl. Acad. Sci. U.S.A. **103:**15599–15604.
568 44. **Jewett TJ, Miller NJ, Dooley CA, Hackstadt T.** 2010. The conserved Tarp actin binding domain
569 is important for chlamydial invasion. PLoS Pathog. **6:**e1000997.
570 45. **Jia TJ, Liu DW, Luo JH, Zhong GM.** 2007. [Localization of the hypothetical protein CT249 in
571 the *Chlamydia trachomatis* inclusion membrane].Wei Sheng Wu Xue Bao **47:**645–648.

572 46. **Jordan IK, Kondrashov FA, Rogozin IB, Tatusov RL, Wolf YI, Koonin EV.** 2001. Constant
573 relative rate of protein evolution and detection of functional diversification among bacterial,
574 archaeal and eukaryotic proteins. Genome Biol. **2:**research0053.
575 47. **Jordan IK, Rogozin IB, Wolf YI, Koonin EV.** 2002. Essential genes are more evolutionarily
576 conserved than are nonessential genes in bacteria. Genome Res. **12:**962-968.
577 48. **Jorgensen I, Valdivia RH.** 2008. Pmp-like proteins Pls1 and Pls2 are secreted into the lumen of
578 the *Chlamydia trachomatis* inclusion. Infect. Immun. **76:**3940–3950.
579 49. **Joseph SJ, Didelot X, Gandhi K, Dean D, Read TD.** 2011. Interplay of recombination and
580 selection in the genomes of *Chlamydia trachomatis*. Biol. Direct. **6:**28.
581 50. **Kanaya S, Yamada Y, Kudo Y, Ikemura T.** 1999. Studies of codon usage and tRNA genes of 18
582 unicellular organisms and quantification of *Bacillus subtilis* tRNAs: gene expression level and
583 species-specific diversity of codon usage based on multivariate analysis. Gene **238:**143– 155.
584 51. **Kari L, Whitmire WM, Carlson JH, Crane DD, Reveneau N, Nelson DE, Mabey DC, Bailey**
585 **RL, Holland MJ, McClarty G, Caldwell HD.** 2008. Pathogenic diversity among *Chlamydia*
586 *trachomatis* ocular strains in nonhuman primates is affected by subtle genomic variations. J. Infect.
587 Dis. **197:**449–456.
588 52. **Kimura M.** 1980. A simple method for estimating evolutionary rate of base substitutions through
589 comparative studies of nucleotide sequences. J. Mol. Evol. **16:**111–120.
590 53. **Kimura M.** 1983. The neutral theory of molecular evolution. Cambridge University Press,
591 London.
592 54. **Le Negrate G, Krieg A, Faustin B, Loeffler M, Godzik A, Krajewski S, Reed JC.** 2008.
593 ChlaDub1 of *Chlamydia trachomatis* suppresses NF-kappaB activation and inhibits IkappaBalpha
594 ubiquitination and degradation. Cell Microbiol. **10:**1879–1892.

595 55. **McDonald JH, Kreitman M.** 1991. Adaptive evolution at the *Adh* locus in *Drosophila*. Nature
596 **351:**652–654.
597 56. **Mehlitz A, Banhart S, Mäurer AP, Kaushansky A, Gordus AG, Zielecki J, Macbeath G,**
598 **Meyer TF.** 2010. Tarp regulates early *Chlamydia*-induced host cell survival through interactions
599 with the human adaptor protein SHC1. J. Cell Biol. **190:**143–157.
600 57. **Misaghi S, Balsara ZR, Catic A, Spooner E, Ploegh HL, Starnbach MN.** 2006. *Chlamydia*
601 *trachomatis*-derived deubiquitinating enzymes in mammalian cells during infection. Mol.
602 Microbiol. **61:**142–150.
603 58. **Mital J, Miller NJ, Fischer ER, Hackstadt T.** 2010. Specific chlamydial inclusion membrane
604 proteins associate with active Src family kinases in microdomains that interact with the host
605 microtubule network. Cell Microbiol. **12:**1235–1249.
606 59. **Mitchell-Olds T, Willis JH, Goldstein DB.** 2007. Which evolutionary processes influence natural
607 genetic variation for phenotypic traits? Nat. Rev. Gen. **8:**845–856.
608 60. **Muller HJ.** 1964. The relation of recombination to mutational advance. Mutat. Res. **106:**2–9.
609 61. **Nei M, Kumar S.** 2000. Molecular Evolution and Phylogenetics. Oxford University Press, New
610 York.
611 62. **Nielsen R.** 2001. Statistical tests of selective neutrality in the age of genomics. Heredity **86:**641–
612 647.
613 63. **Nunes A, Gomes JP, Mead S, Florindo C, Correia H, Borrego MJ, Dean D.** 2007.
614 Comparative expression profiling of the *Chlamydia trachomatis* pmp gene family for clinical and
615 reference strains. PLoS One **2:**e878.

64. **Nunes A, Nogueira PJ, Borrego MJ, Gomes JP. 2010.** Adaptive evolution of the *Chlamydia trachomatis* dominant antigen reveals distinct evolutionary scenarios for B- and T-cell epitopes: worldwide survey. PLoS One **5:**e13171.

65. **Read TD, Brunham RC, Shen C, Gill SR, Heidelberg JF, White O, Hickey EK, Peterson J, Utterback T, Berry K, Bass S, Linher K, Weidman J, Khouri H, Craven B, Bowman C, Dodson R, Gwinn M, Nelson W, DeBoy R, Kolonay J, McClarty G, Salzberg SL, Eisen J, Fraser CM.** 2000. Genome sequences of *Chlamydia trachomatis* MoPn and *Chlamydia pneumoniae* AR39. Nucleic Acids Res. **28:**1397–1406.

66. **Rockey DD, Scidmore MA, Bannantine JP, Brown WJ.** 2002. Proteins in the chlamydial inclusion membrane. Microbes Infect. **4:**333–340.

67. **Saitou N, Nei M.** 1987. The neighbor-joining method: A new method for reconstructing phylogenetic trees. Mol. Biol. Evol. **4:**406–425.

68. **Scidmore-Carlson MA, Shaw EI, Dooley CA, Fischer ER, Hackstadt T.** 1999. Identification and characterization of a *Chlamydia trachomatis* early operon encoding four novel inclusion membrane proteins. Mol. Microbiol. **33:**753–765.

69. **Sharma J, Zhong Y, Dong F, Piper JM, Wang G, Zhong G.** 2006. Profiling of human antibody responses to *Chlamydia trachomatis* urogenital tract infection using microplates arrayed with 156 chlamydial fusion proteins. Infect. Immun. **74:**1490–1499.

70. **Sharp PM, Tuohy TM, Mosurski KR.** 1986. Codon usage in yeast: cluster analysis clearly differentiates highly and lowly expressed genes. Nucleic Acids Res. **14:**5125–5143.

71. **Sisko JL, Spaeth K, Kumar Y, Valdivia RH.** 2006. Multifunctional analysis of *Chlamydia*-specific genes in a yeast expression system. Mol. Microbiol. **60:**51–66.

638 72. **Starnbach MN, Loomis WP, Ovendale P, Regan D, Hess B, Alderson MR, Fling SP.** 2003. An
639 inclusion membrane protein from *Chlamydia trachomatis* enters the MHC class I pathway and
640 stimulates a CD8+ T cell response. J. Immunol. **171:**4742–4749.
641 73. **Stephens RS.** 2002. *Chlamydiae* and evolution: A billion years and counting. In *Chlamydial*
642 Infections: Proceedings of the 10th International Symposium on Human Chlamydial Infections:
643 16-21 June, 2002; Antalya, Turkey Edited by: Schachter J, Christiansen G, Clarke IN, Kattenboeck
644 B, Kuo CC, Rank RG, Ridgway GL, Saikku P, Stamm WE, Stephens RS, Summersgill JT, Timms
645 P, Wyrick PB. San Francisco: International Chlamydia Symposium; 3-12.
646 74. **Stephens RS, Kalman S, Lammel C, Fan J, Marathe R, Aravind L, Mitchell W, Olinger L,**
647 **Tatusov RL, Zhao Q, Koonin EV, Davis RW.** 1998. Genome sequence of an obligate
648 intracellular pathogen of humans: *Chlamydia trachomatis*. Science **282:**754–759.
649 75. **Subtil A, Delevoye C, Balañá ME, Tastevin L, Perrinet S, Dautry-Varsat A.** 2005. A directed
650 screen for chlamydial proteins secreted by a type III mechanism identifies a translocated protein
651 and numerous other new candidates. Mol. Microbiol. **56:**1636–1647.
652 76. **Tamura K, Peterson D, Peterson N, Stecher G, Nei M, Kumar S.** 2011. MEGA5: molecular
653 evolutionary genetics analysis using maximum likelihood, evolutionary distance, and maximum
654 parsimony methods. Mol. Biol. Evol. **28:**2731–2739.
655 77. **Tan C, Hsia RC, Shou H, Carrasco JA, Rank RG, Bavoil PM.** 2010. Variable expression of
656 surface-exposed polymorphic membrane proteins in in vitro-grown *Chlamydia trachomatis*. Cell
657 Microbiol. **12:**174 –187.
658 78. **Tan C, Hsia RC, Shou H, Haggerty CL, Ness RB, Gaydos CA, Dean D, Scurlock AM, Wilson**
659 **DP, Bavoil PM.** 2009. *Chlamydia trachomatis*-infected patients display variable antibody profiles
660 against the nine-member polymorphic membrane protein family. Infect. Immun. **77:**3218–3226.

79. **Thomson NR, Holden MT, Carder C, Lennard N, Lockey SJ, Marsh P, Skipp P, O'Connor CD, Goodhead I, Norbertzcak H, Harris B, Ormond D, Rance R, Quail MA, Parkhill J, Stephens RS, Clarke IN.** 2008. *Chlamydia trachomatis*: genome sequence analysis of lymphogranuloma venereum isolates. Genome Res. **18:**161–171.

80. **Vos M.** 2009. Why do bacteria engage in homologous recombination? Trends Microbiol. **17:**226–232.

81. **Wang J, Chen L, Chen F, Zhang X, Zhang Y, Baseman J, Perdue S, Yeh IT, Shain R, Holland M, Bailey R, Mabey D, Yu P, Zhong G.** 2009. A chlamydial type III-secreted effector protein (Tarp) is predominantly recognized by antibodies from humans infected with *Chlamydia trachomatis* and induces protective immunity against upper genital tract pathologies in mice. Vaccine **27:**2967–2980.

82. **Yang Z.** 1998. Likelihood ratio tests for detecting positive selection and application to primate lysozyme evolution. Mol. Biol. Evol. **15:**568–573.

83. **Yang Z.** 2007. PAML 4: a program package for phylogenetic analysis by maximum likelihood. Mol. Biol. Evol. **24:**1586–1591.

84. **Yang Z, dos Reis M.** 2011. Statistical properties of the branch-site test of positive selection. Mol. Biol. Evol. **28:**1217–1228.

85. **Yang Z, Nielsen R.** 2002. Codon-substitution models for detecting molecular adaptation at individual sites along specific lineages. Mol. Biol. Evol. **19:**908–917.

86. **Yang Z, Nielsen R.** 2000. Estimating synonymous and nonsynonymous substitution rates under realistic evolutionary models. Mol. Biol. Evol. **17:**32–43.

87. **Yang Z, Wong WS, Nielsen R.** 2005. Bayes empirical Bayes inference of amino acid sites under positive selection. Mol. Biol. Evol. **22:**1107–1118.

684 88. **Zhang J, Nielsen R, Yang Z.** 2005. Evaluation of an improved branch-site likelihood method for
685 detecting positive selection at the molecular level. Mol. Biol. Evol. **22:**2472–2479.

686

687

688 **FIGURE LEGENDS**

689 **FIG 1** Chromosomal mapping of *loci* involved in the directional evolution of *Chlamydia trachomatis.*
690 From the outside in, the first and second circles (light blue lines) refer to forward and reverse coding
691 regions, respectively, according to the published genome of the *C. trachomatis* strain D/UW3. The 75
692 evolutionary informative genes evaluated in the present study are highlighted by dark blue lines. These
693 *loci* encompass about 55% of SNPs occurring within the chromosomal coding regions. The third
694 (orange lines) and forth circles (red lines) illustrate genes found to be under positive selection by the
695 codon-based Z-test of positive selection (MEGA5) or the branch-site test of positive selection (PAML),
696 respectively. Circle five shows the GC skew plot. The origin of replication (ORI) and the termination
697 region (TER) are also marked. The figure was built using DNAPlotter (16).

698

699 **FIG 2** Evidence for Muller's ratchet phenomenon. These graphs show nonsynonymous *versus*
700 synonymous mutational dynamics on the *C. trachomatis*/*C. muridarum* separation process. The
701 scattering plot depicts the results concerning the evaluation of nonsynonymous and synonymous
702 substitutions within the *C. trachomatis* species (open circles) (reflecting polymorphism) and between
703 the species *C. trachomatis* and *C. muridarum* (crosses) (reflecting divergence). Neutrality line is also
704 shown. The box plots display the dispersion of the overall decays in the d_N and d_S values [i.e.,
705 d_N(divergence)/d_N(polymorphism) and d_S(divergence)/d_S(polymorphism), respectively]. Outliers and
706 extreme values are marked with open circles and asterisks, respectively. The considerable lower decay

values for d_N suggests that the accumulation of deleterious mutations among strains from *C. trachomatis* species results from genetic bottleneck due to niche restriction (Muller's ratchet effect).

FIG 3 d_N *versus* d_S by gene functional category. This graph represents d_N and d_S values estimated for each gene for all 59 *C. trachomatis* strains. Housekeeping genes (HKs), genes encoding well-known cell envelope proteins (CEPs), genes coding for proteins secreted into the cytosol of the host cells or to the inclusion membrane (SEC), and "other genes" (see methods and Table S2 for details) are represented by squares, circles, triangles, and crosses, respectively. Neutrality line is also shown.

FIG 4 Genetic variability *versus* type of mutation. Distribution of d_N (triangles) and d_S (circles) values according to the nucleotide polymorphism (mean genetic p-distance) of the 75 genes under evaluation among *C. trachomatis* strains. Slope values of the trend lines show a near four-fold higher increase of d_S with p-distance than of d_N.

FIG 5 Non-random distribution of both nonsynonymous and synonymous mutations according to tropism and ecological success. The 3D scatter plot shows the genetic distances between each of the 59 strains and the three disease groups by both d_N (grey) and d_S (black) estimations. Values were estimated by using the concatenated sequences enclosing all genes under evaluation. Strains infecting mononuclear phagocytes (shown in the bottom of the cube), the columnar epithelial cells of ocular (shown in the left side) or genital mucosae compose three major clusters for both d_S and d_N. Within the non-invasive genital strains, the more clinically prevalent strains (labeled with an ellipse) are clustered apart.

730 **FIG 6** Positive selection driving the directional *C. trachomatis* evolution towards niche-specific
731 adaptation. The figure represents a model tree encompassing all 59 *C. trachomatis* strains that was
732 created to facilitate a proper visualization of all biological hypotheses. These evaluate the existence of
733 genes under positive selection (through the branch-site test of positive selection) that may be involved
734 in: specific cell-appetence to columnar epithelial cells of ocular (H1) (serovars A-C) or genital mucosae
735 (H2) (serovars D-K), and to mononuclear phagocytes (H3) (serovars L1-L3); pathogenic diversity
736 among strains causing ocular disease (H4), genital disease (H5), or hemorrhagic proctitis and
737 suppurative lymphadenitis (H6). This test was applied to each individual gene tree in an independent
738 manner for each hypothesis depending of the tree topology. The figure boxes show the genes found to
739 be positively selected for each biological hypothesis. The likelihood-ratio test (LRT) was used for
740 inferring the statistic significance (p-values) of positive selection in the foreground branches. ** and *
741 indicate significance with $p < 0.01$ and $p < 0.05$, respectively. [§] refers to genes presenting congruent
742 trees, but for which a specific biological hypothesis may be affected by recombination (49). See Table
743 1 for details on positively selected codons.
744
745 TABLE 1 Positively selected genes and the inferred codons putatively involved in specific adaptive
746 evolution based on the branch-site test of positive selection by PAML.

ORF [a] (gene)	**Biological hypothesis with positive selection (H1 to H6) [b]**	**p-value (LRT test) [c]**	**Specific codons under positive selection [d, e]**	**Putative function / experimental evidences**	**Specific biological hypothesis excluded due to putative recombination [f]**
CT050	H1	$p < 10^{-10}$	n/d	Pmp-like protein identified in the inclusion lumen (48, 71).	H2, H5
	H3	0.0352	51K*, 80K*, 366K*, 523S*, 546K*		

	H6	$p < 10^{-7}$	183N*, 184S*, 223D**		
CT051	H3	0.0004	563V*	Pmp-like protein (48, 71).	H2, H5
	H6	0.0002	435R**		
CT105	H2	0.0004	n/d	Function unknown.	---
CT115 (*incD*)	H1	$p < 10^{-4}$	11D**, 12G*	Inc (68). T3SS effector (75).	H2, H5
	H3	$p < 10^{-9}$	150L*, 151E*, 153S*, 155S**		
CT147	H3	$p < 10^{-5}$	1407I*	Inc; human early endosomal antigen 1 (EEA1) homologue (8). Immunodominant antigen (69). Involvement in pathogenic differences *in vivo* (51).	H1, H2, H4, H5
	H6	0.0003	n/d		
CT222	H3	$p < 10^{-7}$	124I*,125S**, 126V**	Inc associated with host kinases in microdomains that interact with the host centrosomes (58).	---
CT223	H3	0.0051	127G*, 206R*	Inc (6). T3SS effector (75). Subversion of intracellular trafficking (25). Host cell cytokinesis blockage (1).	---
	H5	0.0082	99R*, 152S*		
CT233 (*incC*)	H6	0.0432	5M*,6S**,7D**,8I*, 11K*, 14I*	Inc (7). T3SS effector (29, 75).	---
CT249	H3	0.0004	8Y*, 24N*, 80T**, 89I**	Inc (45). T3SS effector (24).	---

CT288	H3	0.0104	n/d	Inc (6). T3SS effector (75).	H1, H2, H4, H5
CT413 (*pmpB*)	H3	0.0015	n/d	Adhesin (38). Antigen (21, 35, 78).	H2, H5
	H4	0.0198	58A*, 75T**, 235A*, 820A*, 947E*, 998A*, 1061N**, 1171T**		
	H6	0.0017	n/d		
CT414 (*pmpC*)	H6	$p < 10^{-6}$	145P*, 544I**,598V**	Adhesin (38). Antigen (21, 35, 78).	H2, H5
CT442 (*crpA*)	H6	0.0154	24A*, 29K**, 48I*, 104I**, 133D*, 137V**	Inc (6). T3SS effector (75). Antigen (72).	---
CT456 (*tarp*)	H1	0.0094	447H*, 978H*	Translocated actin-recruiting phosphoprotein / early T3SS effector (20). Contribution for the pathogen phagocytosis(44). Involvement in pathogenic differences *in vivo* (51). Antigen (30, 81).	---
	H3	$p < 10^{-24}$	n/d		
	H4	0.0049	n/d		
	H5	$p < 10^{-8}$	189A**, 237G*, 407S*, 481A**		
	H6	$p < 10^{-28}$	134N*, 139I**, 252G**, 301D*, 351D**, 399G*, 404D**, 493D**[§], 494D*[§], 530K*, 577R*, 603A*, 888G*, 891D**, 909K*		
CT529	H3	0.0009	3A*	Inc (31). T3SS effector (75). Antigen (31, 81).	---

CT622	H3	0.0012	n/d	Involvement in pathogenic differences *in vivo* (51). T3SS effector (37). Antigen (21, 30).	H1, H2, H4, H5
CT694	H? [g]	0.0190	n/d	Immunodominant antigen (21, 69). Early T3SS effector (40). Modulation of host cell processes (10).	---
CT852 (*yhgN*)	H3	$p < 10^{-4}$	202M**, 203L*	Putative integral membrane protein (79).	H2, H5
CT859 (*ispH*)	H3	0.0135	n/d	4-hydroxy-3-methylbut-2-enyl diphosphate reductase (74).	H2, H5
CT867	H3	0.0141	n/d	Deubiquitinase and deneddylase (57).	H1, H2, H4, H5
CT868	H3	0.0064	n/d	Deubiquitinase and deneddylase (57)	H1, H2, H4, H5
	H6	$p < 10^{-5}$	9S**, 17R**, 26S**, 30R**, 105T**[§], 136D**, 138L**, 157Q**, 158T**, 222P**, 238R**, 244V**, 256S**, 287R**, 300P**, 303N**, 307E**, 311F**, 322Y**, 323D**, 324S**, 325K**, 339R**, 340G**, 343S**, 354H**, 358K**, 361L**	Involvement in pathogenic differences *in vivo* (51). Inhibition of a crucial pathway for host inflammatory responses (54).	
CT869	H1	0.0348	59N*, 139I*, 469A*	Adhesin (38).	H2, H5

(*pmpE*)				Antigen (35, 78).	
CT870 (*pmpF*)	H1	$p < 10^{-4}$	n/d	Adhesin (38). Antigen (15).	---
	H3	0.0020	n/d		
CT871 (*pmpG*)	H3	0.0082	n/d	Adhesin (38). Antigen (21, 35, 78).	H2, H5
	H6	$p < 10^{-4}$	258G*, 320K*, 324S*, 812Q**		
CT872 (*pmpH*)	H5	0.0303	n/d	Adhesin (38). Antigen (21, 78).	---
	H6	0.0302	n/d		

747 [a] Open reading frame (ORF) numbers are based on genome annotation of the strain D/UW3 (GenBank
748 No. NC_000117).

749 [b] The hypotheses were created to evaluate the existence of genes under positive selection involved
750 particular biological processes: specific cell-appetence to columnar epithelial cells of ocular (H1) or
751 genital mucosae (H2), and to mononuclear phagocytes (H3); pathogenic diversity among strains
752 causing ocular disease (H4), genital disease (H5), or hemorrhagic proctitis and suppurative
753 lymphadenitis (H6).

754 [c] The likelihood-ratio test (LRT) was used for inferring the statistic significance of positive selection in
755 the foreground branches (p-value). The degree of freedom is 1 for the comparisons of alternative
756 hypothesis versus the null hypothesis in the branch-site test 2.

757 [d] The posterior probabilities that each site belongs to the site class of positive selection on the
758 foreground lineages are inferred by the Bayes Empirical Bayes (BEB) analysis. Positively selected sites
759 are those with ** $p > 0.99$ and * $p > 0.95$. n/d, not discriminated: an excess of positively selected
760 codons hampered their discrimination by PAML, or the identified codons revealed $p < 0.95$.

761 [e] For simplification purposes, amino acid positions for biological hypotheses H1 and H4 are based on
762 the protein sequence annotation for the strain A/Har13, whereas for H2 and H5 are based on the

763 annotation for strain D/UW3, and for H3 and H6 refer to strain L2/434. Within CT456/*tarp* and CT868,
764 the position of the codons labeled with [§] referred to strain L1/1322/p2 as L2/434 is deleted in this
765 region.
766 [f] Recombination was detected in previous studies (39, 41, 49).
767 [g] This gene was detected to be under positive selection specifically for the most clinically prevalent
768 genital strains (mostly from E and F serovars).
769
770
771
772
773
774
775

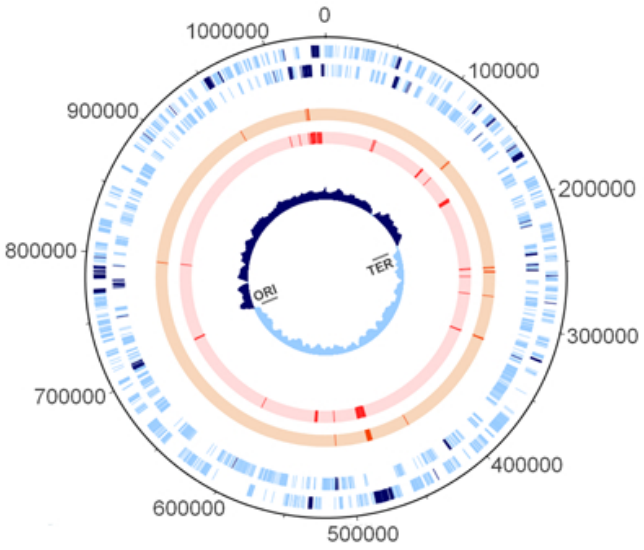

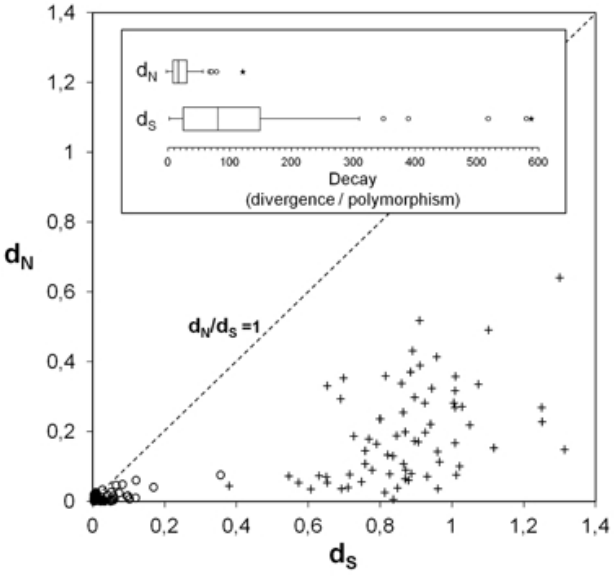

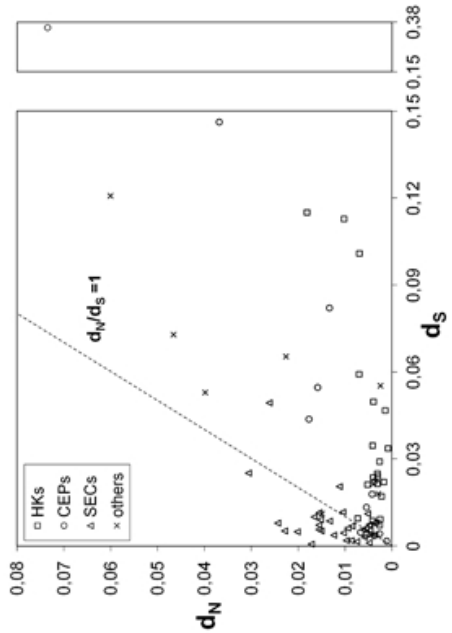

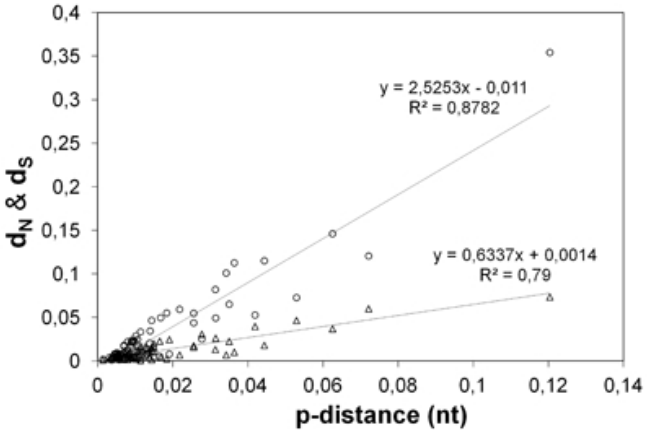

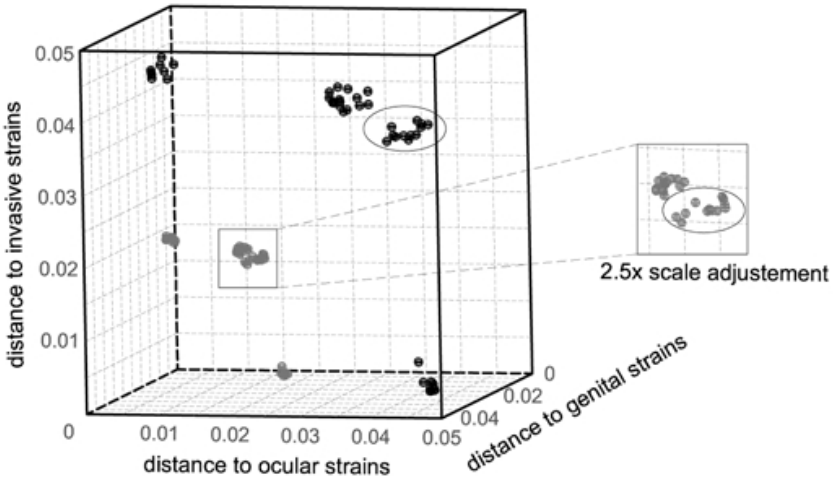

H1

CT050 **
CT115 (*incD*)**
CT456 (*tarp*) **
CT869 (*pmpE*) *
CT870 (*pmpF*) **

H2

CT105 **

H3

CT050 *
CT051 **
CT115 (*incD*) **
CT147 **
CT222 **
CT223 **
CT249 **
CT288 *
CT413 (*pmpB*) **
CT456 (*tarp*) **
CT529 **
CT622 **
CT852 (*yhgN*) **
CT859 (*ispH*) *
CT867 *
CT868 **
CT870 (*pmpF*) **
CT871 (*pmpG*) **

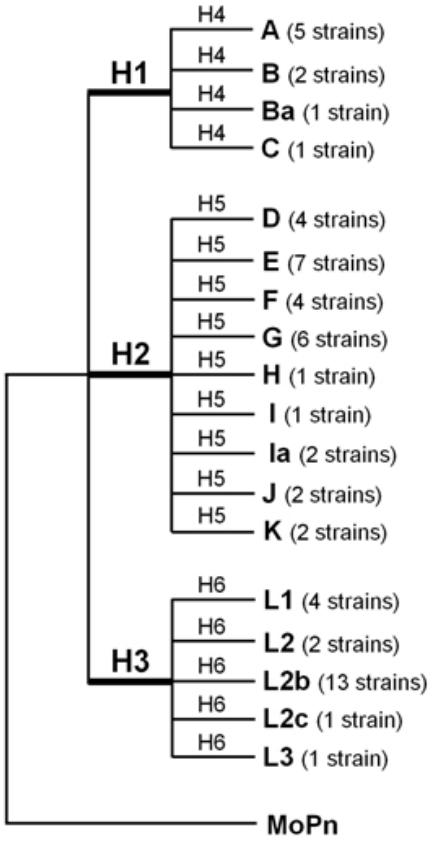

H4

CT413 (*pmpB*) *
CT456 (*tarp*) **, §

H5

CT223 **
CT456 (*tarp*) **, §
CT872 (*pmpH*) *, §

H6

CT050 **
CT051 **
CT147 **
CT233 (*incC*) *
CT413 (*pmpB*) **
CT414 (*pmpC*) **
CT442 (*crpA*) *
CT456 (*tarp*) **, §
CT868 **
CT871 (*pmpG*) **
CT872 (*pmpH*) *, §